

INFERRING THE COMPOSITION OF SUPER-JUPITER MASS COMPANIONS OF PULSARS WITH RADIO LINE SPECTROSCOPY

ALAK RAY^{1,2‡}, ABRAHAM LOEB^{1†}

¹Institute of Theory and Computation, Center for Astrophysics, Harvard University
60 Garden Street, Cambridge, MA 02138 and

²Tata Institute of Fundamental Research, Homi Bhabha Road, Mumbai 400005, India

Draft version August 6, 2018

ABSTRACT

We propose using radio line spectroscopy to detect molecular absorption lines (such as OH at 1.6-1.7 GHz) before and after the total eclipse of black widow (BW) and other short orbital period binary pulsars with low mass companions. The companion in such a binary may be ablated away by energetic particles and high energy radiation produced by the pulsar wind. The observations will probe the eclipsing wind being ablated by the pulsar and constrain the nature of the companion and its surroundings. Maser emission from the interstellar medium stimulated by a pulsar beam might also be detected from the intrabinary medium. The short temporal resolution allowed by the millisecond pulsars can probe this medium with the high angular resolution of the pulsar beam.

Subject headings: (stars:) pulsars: general – (stars:) binaries: eclipsing – radio lines: planetary systems – interplanetary medium – ISM: molecules – masers – shock waves

1. INTRODUCTION

The first set of planets orbiting any star other than our Sun were discovered around a millisecond pulsar ($P_{spin} = 6.2$ ms) PSR B1257+20 at a distance of 600 pc (Wolszczan and Frail 1992). The discovery and follow-up of a similar class of pulsars with low mass companions, namely the black widow (hereafter ‘BW’) pulsars¹, also led to questions of how planets could form or remain around rapidly rotating pulsars (Podsiadlowski 1993). It has been argued that the most plausible scenarios for the formation of these planets involve a disk of gas around the pulsar (Phinney & Hansen 1993). However a search for these debris disks around several pulsars such as PSR B1257+20 (Foster and Fischer 1996) from space and ground-based observatories yielded no detections (Lazio and Fischer 2004; Wang et al 2014).

The composition of planets and their atmospheres around main sequence stars has emerged as a key area in exoplanet research especially after the Kepler and COROT missions (see Madhusudhan et al (2014) and references therein). The discovery of the original black widow pulsar PSR B1957+20 (Fruchter et al 1988, 1990), a millisecond radio pulsar ablating its companion in a binary system ($P_{orb} = 9.17$ hr), showed that gas in the eclipsing region is being continually replenished from the companion’s extended atmosphere (see Fig. 1). The 1.61 ms pulsar disappears behind the companion in a wide eclipse for $\sim 10\%$ of its binary orbit. The companion has a very low mass ($M_c \sim 0.025 M_\odot$) and the eclipsing region is substantially larger than the Roche lobe of the companion. Kluzniak et al (1988); Phinney et al (1988) suggested that strong gamma-ray irradiation from the millisecond pulsar drives the wind from the companion star and gives rise to a bow shock between the wind and

pulsar magnetic field at a distance of roughly ($0.7R_\odot$) from the companion around which the plasma is opaque to radio waves of frequencies ≤ 400 MHz. The pulsar may be left as an isolated millisecond pulsar as in PSR B1937+21 after few times 10^8 yr. The observability of these binary pulsars in the black widow state implies that the lifetime of this transitory phase cannot be much shorter. Given the strong pulsar radiation and the relativistic electron-positron outflow ablating its companion to drive a comet-tail like wind, it is feasible to search for absorption lines in radio spectra. Such lines in absorption spectroscopy or maser emission in the interstellar medium (ISM) has already been detected for several pulsars (Stanimirovic et al. 2003; Weisberg et al 2005). In this paper, we explore the prospects of detecting the composition of the gas evaporated from the very low mass companion of the neutron star, which may in turn lead to a better understanding of the past evolutionary history of such systems as well as probe the composition of the companions themselves. This in turn could constrain the formation scenarios of ultra-low mass companions of pulsars.

2. BLACK WIDOW AND RED BACK PULSARS IN THE GALACTIC FIELD AND GLOBULAR CLUSTERS

The advent of the large area gamma-ray telescopes like *Fermi* soon led to the discovery of a large population of short period millisecond pulsars (Caraveo 2014) that has dramatically increased the number of black widow like systems similar to PSR B1957+20 (Roberts 2013). The list compiled by Roberts (2013) was recently supplemented by PSR J1311-3430 (BW) (Romani 2012) and PSR J2339-0533 (RB) (Ray, P. S. et al. (2014) and Ray et al (2015, in preparation)). Red back pulsars (hereafter ‘RB’) like the black widows are eclipsing millisecond pulsars with relatively short orbital periods ($P_B < 1$ d), but have slightly more massive companions ($0.1 M_\odot < m_c < 0.4 M_\odot$) compared to black widow pulsars. PSR J1023+0038 is the prototype red back pulsar in the Galactic field. It is a 1.69 ms pulsar in a 4.8 h or-

[‡] akr@tifr.res.in

[†] aloeb@cfa.harvard.edu

¹ These are defined as a class containing eclipsing binary millisecond pulsars with ultra-low mass companions

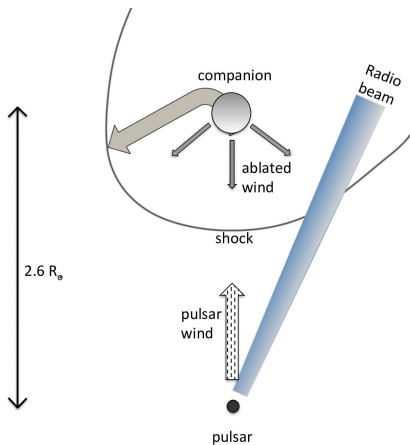


FIG. 1.— Sketch of the geometry for a pulsar beam passing through the ablated wind from the super-Jupiter companion orbiting a black widow pulsar. The fiducial value of $2.6R_{\odot}$ for the companion’s orbital radius is characteristic of PSR B1957+20 where the inferred radius of the eclipsing region $R_E = (f_w c/v_w)^{1/2} R_2 = 0.7 R_{\odot}$, where f_w is the fraction of the incident spin down power on the companion that is carried off in the form of the wind, v_w is the wind speed, and R_2 is the radius of the ablating companion (Phinney et al. 1988). This is a representative case amongst systems with different orbital periods, pulsar spin down power, and wind parameters. The wind may be rich in Oxygen if the companion is the remnant of a star that has generated Carbon or Oxygen during its own evolutionary process.

bit around a companion star of mass $0.2 M_{\odot}$ whose radio pulsations confirmed it to be a neutron star (Archibald et al. 2009). Like PSR B1957+20, its eclipse durations are also dependent on the radio frequency of observation. Its optical studies combined with Very Long Baseline Interferometry (VLBI) observations implied that its companion was close to filling its Roche lobe and is non degenerate, and suggested that the red backs represented a system where the neutron star is recently recycled and the accretion² is temporarily halted revealing the radio pulsar which begins to ablate the companion (Bogdanov et al. 2015; Benvenuto et al. 2015; Chen et al. 2013). PSR J1023+0038 is considered a “transitional” red back system since it shows transitions between accretion- and rotation-powered states and belongs to both classes of red back radio pulsars and transient low mass X-ray binaries (LMXBs). This pulsar provides direct support for the formation and spinup scenario of millisecond pulsars due to transfer of angular momentum due to accretion of matter on to the neutron star from its companion star (Alpar et al. 1982; Radhakrishnan & Srinivasan 1982). It is the first of this subclass of red backs (the others are: PSR J1824-2452I, PSR J1227-4853 (Roy et al. 2015) and the “candidate” transitional pulsar PSR J1723-2837 (Bogdanov et al. 2014). Black widow and red back pulsars are found also in globular clusters³. If the requirement for an eclipse is relaxed, then there are almost as many millisecond pulsars with ultra-low mass compan-

² This system showed double peaked emission lines in the optical spectrum obtained in Sloan Digital Sky Survey in 2001 indicating the presence of an accretion disk around the neutron star (Wang et al. 2009). Whether red back pulsars evolve to black widow pulsars is however debated (see Jia & Li (2015); Benvenuto et al. (2015)).

³ See Paolo Freire’s compilation (Freire 2012) of properties of pulsars in globular clusters: www.naic.edu/~pfreire/GCpsr.html

ion (23) in a globular cluster as compared to those in the Galactic field (22). In the binary containing PSR J1824-2452I in globular cluster M28 there is the transition of the opposite kind which was first observed as a rotation powered pulsar but then swung to an accretion powered low luminosity X-ray millisecond pulsar (Papitto et al. 2013). High states of γ -ray emission in the red back PSR J1227-4853 are explained by the Comptonization of disc radiation to GeV energies by secondary electrons produced in the pulsar slot-gap (Bednarek 2015). Because of their ever-changing accretion these pulsars may offer interesting insights towards the formation and evolution of millisecond pulsars in general and of systems with planetary or ultralow mass companions.

For black widows in globular clusters, King et al. (2003) invoked a two step process, in which cluster turn-off mass stars exchange into wide binaries containing recycled millisecond pulsars and remnant helium white dwarf of the donor star, exchanging itself for the white dwarf and ejecting the latter. Subsequently, the new companions overflow their Roche lobes because of encounters and tidal dissipation. The rapidly spinning neutron stars eject the overflowing gas from the system on a relatively rapid time-scale at first. The systems enter an observable black widow phase at epochs when the evolution is slow, so that the corresponding lifetime is long and the probability of finding the system in this phase is substantial, and the mass loss is small enough to make the environment transparent to radio waves. The incidence of known evaporating black widow pulsars among the binary millisecond pulsars in globulars and the galactic field are comparable. The King et al. (2003) scenario requires high temperature gas present in the intra and circumbinary region where all molecules would be dissociated. However, Wasserman & Cordes (1988) argued the gas temperature to be decreasing adiabatically with distance from the companion and argued for a much lower temperature for the gas surrounding the companion of PSR 1957+20 (see below). Therefore, detection of a molecular lines from these systems will invalidate the high temperature models. Unfortunately amongst the pulsars where L-band flux has been reported, the radio flux density in the 1.6 GHz band for molecular line detection from almost all black widow and red back pulsars in globular clusters are too low to be observable with the current generation of radio telescopes, except possibly PSR J1807-2459A, but several may become detectable with the greater sensitivity of the Square Kilometer Array (SKA).

Bailes et al (2011) have discovered a millisecond pulsar PSR J1719-14 in a very close binary system ($P_{orb} = 2.2$ hr) whose companion has a mass near that of Jupiter, but its minimum density suggests that it may be an ultralow mass carbon white dwarf. This system does not show any evidence of solid body eclipses or excess dispersive delays perhaps due to an unfavorable angle of inclination of its orbit relative to our line of sight. Nevertheless, its discovery points to the existence of systems which may have once been an ultra compact low mass x-ray binary where the companion has narrowly escaped complete evaporation. Similar systems with more favorable inclination angles may be discovered in future surveys with wider coverage and computational analysis power

expected in the SKA⁴ era and will be of interest for the reasons we discuss next.

3. PLANETS AROUND PULSARS, THEIR EVAPORATION AND INTRABINARY GAS

Since the discovery of the first extra-solar planet around PSR B1257+12 (Wolszczan and Frail 1992) there has been only one other radio astronomical discovery of a super-Jupiter planet in a triplet system within a globular cluster namely PSR B1620-26 (Thorsett et al. 1993; Richer et al. 2003; Sigurdsson et al. 2003). Despite sensitive monitoring of more than 151 young ($\tau < 2$ Myr), luminous pulsars for periodic variation in pulse arrival time due to possible planetary companions, Kerr et al (2015) failed to detect any further planetary companions around pulsars. However these pulsars are not only young and slow rotators, but their pulse timing properties are usually far less accurate than that for old millisecond pulsars hosted by black widow systems. It is therefore possible that in addition to the causes mentioned by Kerr et al (2015) the search could have been less sensitive for planets around normal pulsars as opposed to those around millisecond pulsars like PSR B1257+12. Podsiadlowski (1993); Phinney & Hansen (1993) classified the various planet formation models for planets around pulsars (especially in the context of PSR B1257+12) into two groups: i) the planets formed around an ordinary star like in our solar system and later on this star exploded and created a spinning neutron star, yet the planets survived, or the planetary system was captured by a neutron star in a direct collision with the solar-type main sequence central star; and ii) the planets formed soon after the pulsar was born in a supernova explosion. Podsiadlowski (1993) suggested a third set of models in which planet formation constitutes the final stage in the evolution of some millisecond pulsars, e.g. the circumbinary disk models, where a binary companion of a millisecond pulsar is being evaporated (Banit et al 1993), or in which the evaporation is taking place in a low mass X-ray binary phase (Tavani and Brookshaw 1992). In contrast to the simple evaporation models, some of the material may not escape from the system and may form a circumbinary disk, from which planet formation can take place.

The environment of the planets around pulsars is characterized by high irradiation of both photons and particles from the millisecond pulsar. Chemistry in this gaseous medium may bear similarities to dense photon dominated regions (Sternberg & Dalgarno 1995), where more energetic photons than far-ultraviolet (FUV) radiation as well as electron and baryonic particle flux may be substantial. As shown by Sternberg & Dalgarno (1995), various gas-phase photochemical processes may lead to the production of atomic and molecular species in dense photon dominated regions. The physical and chemical properties of photon dominated regions in a dense molecular cloud depend upon the gas density and pressure, intensity of high energy radiation, gas phase elemental abundances and the presence of dust grains. Sternberg & Dalgarno (1995) showed that OH , H_2O

and their ionic forms or their precursor molecule H_3O^+ may form in both photon mediated as well as electron mediated processes in hot HI zone and near the H/H_2 transition layer (see section 3.1.1 of their paper). They employed models involving a static, plane parallel, semi-infinite cloud exposed on one side to an isotropic radiation field with a constant hydrogen particle density $n_T = n_H + n_{H_2} = 10^6 \text{ cm}^{-3}$ throughout the cloud and an incident FUV field with an intensity 2×10^5 times the average interstellar FUV field estimated by Draine (1978). They found that the OH abundance, a crucial intermediary in the chemistry of the hot gas that leads to the production of many molecules and molecular ions, reaches a maximum at a visual extinction $A_V = 0.6$ where the gas temperature is 800 K. In fact their density ratio with respect to H_2O , OH/H_2O dominates even at higher visual extinctions up to $A_V = 3$ in the clouds. With the assistance of reactions on grain surfaces, hydrogen molecules form by the association of hydrogen atoms and the neutral hydrogen HI gas is hot with temperatures exceeding 10^3 K at a depth $A_V = 0.7$ from the cloud surface. This is because the gas heating by grain photoelectric emission and collisional de-excitation of energetic radiation-pumped H_2 becomes efficient while emission cooling is quenched (Sternberg & Dalgarno 1995; Burton et al. 1990).

The environment of a pulsar which resulted from a supernova explosion is likely to be particularly rich in metals. Grain formation can take place in metal rich gaseous surroundings of the pulsar and its planet. Much of the chemistry in planet forming regions around normal stars has been shown recently to be driven by gas-grain chemistry. The smaller grains of size between $0.001\mu\text{m}$ and $0.1\mu\text{m}$ which provide most of the surface area for chemistry are critical for absorption and scattering of UV radiation (van Dishoeck 2014). Interstellar grains are agents through which surface molecules participate in promoting the reaction rather than having an active role as catalysts. Primarily, they provide a reservoir where atoms and molecules can be stored and brought closer together for much longer periods than probable in the gas phase and can enable reactions that are too slow with substantial activation barriers. Additionally, by acting as a third body that absorbs the binding energy of the newly formed molecule, they stabilize it from dissociating quickly. As in canonical planetary systems, long lived pulsars with ultra-low mass companions may have disks where grains form and assist molecule formation.

4. RADIO ABSORPTION SPECTROSCOPY OF ABLATED GAS FROM THE PLANET OR COMPANION OBJECT

The time dependent nature of the pulsar emission offers an advantage: the narrow beam of pulsar radiation makes a pencil sharp probe of the intervening medium especially if it gives rise to an absorption dip in the pulsar continuum. The pulsar “on” spectrum represents the signal of the pulsar alone as modified by absorption and in rare circumstances by stimulated emission (Weisberg et al 2005) by the intervening medium in a narrow angle. In contrast, the pulsar “off” spectrum in the intervening time between the pulses has both line emission and absorption occurring within the wider telescope beam. Given the flux density of most pulsars fall off

⁴ See Keane et al. (2015); Tauris et al. (2015) in The SKA Key Science Workshop Documentation at: <http://astronomers.skatelescope.org/meetings-2/2015-science-meeting/>

TABLE 1
BLACK WIDOW AND OTHER PULSAR TARGETS FOR OH LINE SPECTROSCOPY^A

Pulsar	l, b deg	P_{spin} ms	W50 ms	P_B hrs	Min. m_c M_{Jup}	Age ^B 10^9 yr	\dot{E} L_{\odot}	D kpc	S_{1400} mJy	Ref.
J2051-0827	39.2, -30.4	4.51	0.34	2.4	28.3	5.61	1.4	1.28	2.8	<i>a, b, c</i>
J2241-5236	237.5, -54.9	2.19	0.07	3.4	12.6	5.22	6.5	0.68	4.1	<i>d</i>
J0751+1807	202.7, -21.1	3.48	0.70	6.3	134 ^D	7.08	1.9	0.40	3.2	<i>d, h, i</i>
J1012+5307	160.3, +50.8	5.25	0.69	14.4	112 ^D	4.86	1.2	0.70	3.0	<i>d, j, k</i>
J1807-2459A ^C	5.8, -2.2	3.06	0.33	1.7	9.4	—	—	2.79	1.1	<i>e, f, g</i>
B1259-63	304.2, -1.0	47	23	1236d	$10M_{\odot}$	3×10^5 yr	207	2.3	1.7	<i>l, f, m</i>
B1957+20	59.2, -4.7	1.61	0.035	9.1	22	2.2	40	1.53	0.4	<i>n, c</i>
J1227-4853 ^F	298.9, +13.8	1.69	—	6.8	221 ^D	2.4	24	2.00	— ^F	<i>r</i>
J1723-2837	357.6, +4.26	1.86	0.20	14.8	247 ^D	3.9	12	1.00	1.1	<i>s</i>

^A Pulsars with moderate *mean* flux density S_{1400} ; from ATNF Pulsar Database (Manchester et al 2005): www.atnf.csiro.au/people/pulsar/psrcat/; PSR B1957+20 is included for comparing parameters

^B Age = $P_{\text{spin}}/2\dot{P}$; \dot{P} uncorrected for Shklovsky effect

^C in Globular Cluster NGC6544; pulsar spindown age and luminosity are uncertain due to acceleration effects

^D these companions correspond to red back pulsars

^F estimated flux in 1.4 GHz band is 1.6mJy using the reported 607 MHz flux and spectral index -1.7 from (Roy et al. 2015)

^a Stappers et al (1996)

^b Doroshenko et al (2001)

^c Kramer et al (1998)

^d Keith et al (2011)

^e Ransom et al (2001)

^f Hobbs et al (2004)

^g Lynch et al (2012)

^h Lundgren et al (1995)

ⁱ Nice et al (2005)

^j Nicastro et al (1995)

^k Lazaridis et al (2009)

^l Johnston et al (1992)

^m Melatos et al (1995)

ⁿ Fruchter et al (1988)

^r Roy et al (2015)

^s Crawford et al (2013)

rapidly with observing radio frequency it is natural to target pulsars for atomic or molecular line transitions in the L- (1.4 GHz) band and possibly in the X- (8-12 GHz) band. Stanimirovic et al. (2003) detected molecular OH absorption against PSR B1849+00 at 1.665 GHz and at 1.667 MHz. In addition, there exist other hyperfine transition lines of $^3\text{He}^+$ ($^2S_{1/2}, F = 0 - 1$) at 8.665 GHz and molecular lines Ortho-Formaldehyde (H_2CO) at 4.83 GHz and of Methanol (CH_3OH) at 6.67 GHz with relatively large Einstein A coefficients (Rohlfs and Wilson 1996). Although the Helium isotope ^3He has an abundance of 1.38×10^{-4} % (^4He abundance is likely to be high in an evolved remnant of companion of the pulsar), since the pulsar spectra decline steeply with frequency, it might be challenging at present to detect these atoms or molecules in absorption or stimulated emission against pulsar radiation.

4.1. Molecular gas: interstellar or in situ binary?

Stanimirovic et al. (2003) and Weisberg et al (2005) detected OH absorption in PSR B1849+00 and PSR B1641-45 using Arecibo and Parkes radio telescopes respectively out of a total of 25 pulsars. In addition Minter (2008) detected OH absorption for PSR B1718-35 by using the Green Bank telescope (GBT) out of a sample of 16 pulsars. While PSR B1641-45 has a relatively large mean flux density of $S_{1400} = 310$ mJy, the other two have 11 mJy (PSR B1718-35) and 2.2 mJy (PSR B1849+00) respectively. Thus, typically only about 10%

of the searched for targets show evidence of OH absorption (or stimulated emission) in pulsar lines of sights. The detections have been made only for low-galactic latitude pulsars (see galactic (l, b) in Table 2). However almost all target pulsars listed in Table 1 turn out to be high galactic latitude pulsars. Since OH is generally strongly confined to the galactic plane, any detection of OH absorption (or stimulated emission) in these systems will be related to the binary system with high probability rather than be interstellar. The intrabinary molecular gas signature can be distinguished from circumbinary molecular gas by the orbital phase modulation (i.e. when the pulsar is near inferior conjunction). Binning the recorded data with respect to companion orbital phase would allow the exclusion of low signal to noise (for molecular gas) in high impact parameter data (when companion orbital position is far away from inferior conjunction). In case of very high signal to noise of atomic/molecular gas in the background of a bright pulsar it may even be possible to study the variation of absorption and emission with the impact parameter which can then lead to information about the radial structure of the ablated wind from the companion. As only times close to the total eclipse would have substantial OH absorption in the trailing wind, only the fraction of the orbit near the eclipse ingress and egress have to be added from multiple orbital cycles.

4.2. OH molecular line absorption towards pulsars

In the context of the black widow PSR B1957+20 one can expect sufficiently large column depths of OH molecules near the eclipsed region, i.e. in orbital phases close to the inferior conjunction to show moderate line absorption with reasonable equivalent width (EW). This is because the gas can cool adiabatically with distance from the ablating companion star (see below) to enable molecule formation. Unfortunately the mean flux density ($S_{1400} = 0.4$ mJy) for this pulsar is too low for an easy detection by existing telescopes. Table 1 lists the characteristics of pulsars that may be suitable for detection of molecular lines through radio spectroscopy. Note that we include here PSR B1957+20 for comparison – because of its very low mean flux density at 1400 MHz it is not meant to be a target for OH detection with the current generation of telescopes. On the other hand PSR B1259-63 has a massive Be star companion which does not belong to the black widow or red back classes but whose high ΔDM post- and pre-eclipse phases last for tens of days during which an OH line spectroscopy can be carried out. Table 2 lists pulsars from which OH line absorption has been observed in the ISM during the pulse “on” phase. For PSR J1641-45, not only line absorption at 1612 MHz, 1665 MHz and 1667 MHz, but even stimulated emission at 1720 MHz driven by the pulsar during its pulse “on” phase has been detected by Weisberg et al (2005). This is the only pulsar, an extremely bright one, from which the stimulated emission was discovered, not among the other fainter ones in Table 2. Therefore, the use of stimulated emission to probe the conditions of the companion’s wind in a binary pulsar may be possible if such an extremely bright pulsar were to be discovered in a binary system. The examples in Table 2 give column depths of OH line absorption already detected against isolated and bright pulsars with existing telescopes in reasonable exposure times. They are “ordinary” pulsars with duty cycles ($= W50/P_{\text{spin}}$) ranging from 1.8% to 10.8%, moderate radio flux densities in the 1400 MHz band close to where the OH line absorption at 1612-1720 MHz band is expected and are young pulsars with spindown power comparable to the solar luminosity. The targets listed in Table 1 are *binary, millisecond* pulsars with high spindown power and moderate radio flux densities at 1400 MHz, with ultra-low mass (or even comparable to Jupiter mass) companions in close orbits ($P_{\text{orb}} \sim 2 - 14$ hr). Note their duty cycles are comparable to those in Table 2 even though they are much more rapidly spinning and their moderate mean flux densities at 1400 (1600) MHz and their small orbital dimensions make them good targets for HI/OH absorption studies against their pulsed flux. Black widows among the entries in Table 1 (the first two) have ultralight companions that are partially degenerate and stripped due to ablation by the pulsar. X-ray studies of black widow pulsars show that their non-thermal X-ray emission are orbitally modulated which has been related to the intrabinary shocks close to the companion (Phinney et al 1988; Roberts 2013).

The eclipse duration in PSR B1957+20 is a function of observing radio frequency. Rasio et al (2012) and Wasserman & Cordes (1988) argued that the radio radiation is being absorbed with a frequency dependent cross section rather than refraction and reflection from ionized plasma wind (Phinney et al 1988). Radio line absorp-

tion in the OH 1.6 GHz band against pulsed flux can be easily associated with interstellar vs in-situ (planetary or intra-binary) origins by the independent evidence of binarity and a correlated change of OH absorption with orbital phase near eclipse ingress and egress.

The observed line intensity profile of OH absorption can be written in terms of the OH column density N_{OH} as (Hewitt et al 2006):

$$I_{\nu} = (1 - f)I_{0\nu} + f\{I_{0\nu} \exp(-\tau_{\nu}) + B_{\nu}(T_{\text{ex}})[1 - \exp(-\tau_{\nu})]\}$$

where $I_{0\nu}$ is the background continuum intensity, represented by the pulsed radio flux during the pulsar “on” phase, $B_{\nu}(T_{\text{ex}})$ is the Planck function, T_{ex} is the excitation temperature of the four transitions that represent the OH molecular lines in the L-band, τ_{ν} is the optical depth at frequency ν and f is a telescope beam filling factor (which we take to be unity as only the pulsar “on” phase is compared with the flux in between the pulses, i.e. “off-pulse”). This can be rewritten in terms of the brightness temperature, assuming that $T_{\text{ex}} \gg h\nu_{OH}/k_B = 0.08$ K where the Rayleigh-Jeans approximation holds:

$$T(v) - T_0 = f(T_{\text{ex}} - T_0)\{1 - \exp[-\tau(v)]\}.$$

Here $\tau(v)$ can be written in terms of the optical depth at the line center τ_0 with a Gaussian profile:

$$\tau(v) = \tau_0 \exp[-(v - v_0)^2/(2\sigma^2)]$$

where the line width σ is related to the velocity dispersion Δv through $\sigma = \Delta v/(8\ln 2)^{1/2}$. The optical depth at the line center depends upon the OH molecular column density N_{OH} , corresponding Einstein A-coefficient, degeneracies of the upper and lower states and the occupation fraction of the initial state, and the excitation temperature T_{ex} and can be collectively written as:

$$\tau_0 = a \frac{N_{OH}(10^{15} \text{ cm}^{-2})}{T_{\text{ex}}(\text{K})\Delta v(\text{kms}^{-1})} \quad (1)$$

with the constant $a = 0.454, 2.345, 4.266$ and 0.485 for the 1612, 1665, 1667 and 1720 MHz lines respectively (see Hewitt et al (2006)). For the strongest “main” line at 1667 MHz, this leads to the column depth:

$$N_{OH} = 2.3 \times 10^{14} \text{ cm}^{-2} (T_{\text{ex}}/\text{K}) \int \tau(v)dv/(\text{kms}^{-1}) \quad (2)$$

As an example, Stanimirovic et al. (2003) obtained for *interstellar* OH absorption against PSR B1849+00, $\tau_{\text{max}} = 0.4 \pm 0.1$ at 1665 MHz and $\tau_{\text{max}} = 0.9 \pm 0.1$ at 1667 MHz with corresponding line-width FWHM of $1.5 \pm 0.4 \text{ km s}^{-1}$ and $1.1 \pm 0.2 \text{ km s}^{-1}$. The corresponding N_{OH}/T_{ex} are tabulated in Table 2.

4.2.1. Eclipsing gas temperature

What is the temperature of the eclipsing gas at a pulsar line of sight impact parameter b ? Here $b = \pi a \Delta\phi$, where a is the radius of the orbit of the planet or ultra-low mass stellar companion and $\Delta\phi \ll 1$ is the orbital phase of the eclipse. In the context of the original black widow pulsar PSR B1957+20, Wasserman & Cordes (1988) found the gas temperature to be ~ 260 K from the dispersion

TABLE 2
PULSARS WITH OH ABSORPTION DETECTED AGAINST PULSED EMISSION

Pulsar	l, b degree	P _{spin} ms	W50 ms	Age ^A 10 ³ yr	\dot{E} L _⊙	D kpc	S ₁₄₀₀ mJy	N _{OH} /T _{ex} 10 ¹⁴ cm ⁻² K ⁻¹	Telescope	Exp. hrs	Ref.
B1641-45	339.2, -0.2	455	8.2	3.59	2.2	4.5	310	0.28 ^B	Parkes	5	1
B1718-35	351.7, +0.7	280	26	1.76	11.8	4.6	11.0	0.1-0.67	GBT	< 10	2
B1849+00	33.5, +0.02	2180	235	3.56	0.1	8.0	2.2	2.7	Arecibo	3.4	3

^A Age = P_{spin}/2 \dot{P} . Note the different units of age used in Table 1.

^B Calculated from $\tau = 0.03$ at 1667 MHz with FWHM $\Delta v = 2 \text{ kms}^{-1}$ reported in Ref. 1.

¹ Weisberg et al (2005)

² Minter (2008)

³ Stanimirovic et al (2003)

measure fluctuations accompanying emission from the eclipse, assuming that the eclipse is caused by free-free optical depth. Temperature is expected to decline adiabatically as $T \propto r^{-4/3}$ with distance r from the companion. Surface temperatures of the companions (the optical counterparts) of a number of black widow and red back pulsars (detected in γ -rays with Fermi Gamma Ray Telescope) were determined by UV and optical observations (Gemini, NTT and Swift-UVOT) by Breton et al. (2013). They measured both “dayside” and “nightside” temperatures (i.e. of the hemispheres of the companion facing the pulsar or on its opposite side). While “nightside” temperatures can be of the order of ~ 2500 K the “dayside” temperatures range between 4200–8000 K. Kaplan et al. (2013) in their Fig 6 compare surface temperatures and gravity of the companions of several black widow and red back pulsars, e.g. in PSR J0751+1807 (with $m_c \sim 0.14M_\odot$) temperature could be as low as 3500 K (Bassa et al. 2006). HST observations of the companion of PSR J2051-0827 have yielded temperatures ~ 2500 K on its unirradiated side in certain orbital phases (Stappers et al. 2001). If the companions are very low mass proto-He white dwarf companions of the millisecond pulsars that may be out of Roche lobe contact for over several Gyr, their radius R_c contracts to $\leq 0.07R_\odot$ (see Fig 3 of Istrate et al. (2014); on the other hand, for a core derived from a main sequence star with cosmic abundance, the companion radius $R_c \sim 0.1R_\odot$ as in the case of PSR B1957+20). With the radius and surface temperature of the He white dwarf companion, gas on the nightside cooling adiabatically with $T \propto r^{-4/3}$ would reach ~ 100 K within a distance $16R_c \sim 1 R_\odot$ from the companion, which is the typical dimension of the eclipsing region in a black widow pulsar (Phinney et al 1988).

4.2.2. OH column depths

To estimate the column depth of N_{OH} from beyond the eclipsing region we may adopt $T_{ex} \sim 100$ K and a line-width of FWHM $\sim 3 \text{ km s}^{-1}$ (see section 5.1). Since the ablated wind from the companion is primarily in the tangential direction, or may reside for long periods in a Keplerian disk centered on the neutron star, the effective velocity width of the radiatively connected region in the line of sight along the pulsar beam may not exceed much the thermal speed. Therefore, a velocity resolution of 1.0 km s^{-1} would sufficiently resolve the absorption profile in several bins. Adopting $\tau_0 = 0.3$ at 1667 MHz (similar to that observed in *interstellar* OH absorption against PSR B1718-35 with a comparable spectral reso-

lution as in Minter (2008)), one requires an intra-system column depth of $N_{OH} = 2.28 \times 10^{16} \times 0.9 \sim 10^{16} \text{ cm}^{-2}$.

We argue that this column density is comparable to what is derived from the mass loss rate from the pulsar companion in a wind outflow:

$$\dot{M}_w = f_\Omega 4\pi\rho r^2 v_w.$$

Here f_Ω is the fraction of the total solid angle covered by the wind ablated from the companion ρ is the mass density in the wind at a distance r from the pulsar and v_w is the speed of the wind being blown out by the pulsar energetic outflow in photons and particles. The column density N_{OH} that radio radiation from the pulsar encounters is:

$$N_{OH} \sim (X_{OH}/m_{OH})\rho \times s.$$

Here, X_{OH} is the OH fraction⁵ in the wind (fraction of the nucleons locked up in OH), whose typical value is $\sim 10^{-3}$, n_X ’s are the number *densities* of the element X, and s is the absorption lengthscale encountered by the pulsar beam in the intrabinary space typically of dimensions comparable to that of the eclipsing region, and m_{OH} is the mass of an OH molecule. For the case of PSR B1957+20, Phinney et al (1988) has argued that the eclipsing region is $\sim 0.7R_\odot$, and so we adopt in our calculations $s \sim r$. The expression above can be further reduced in terms of parameters of the pulsar system under consideration by the equating the timescale of complete ablation of the planetary mass companion to the spin down timescale for the pulsar:

$$N_{OH} = \frac{\dot{M}_w X_{OH} s}{f_\Omega 4\pi\rho r^2 v_w m_{OH}}. \quad (3)$$

In terms of the parameters of PSR B1957+20 with an

⁵ The Solar Oxygen nucleon fraction is $X_O = 5.5 \times 10^{-3}$ using the scaling $n_O/n_H = 4.89 \times 10^{-4}$ from $\log \epsilon_O = 8.69$ (Asplund et al 2009) with the definition: $\log (n_X/n_H) + 12 = \log \epsilon_X$.

assumed evaporation timescale⁶ yields a column density,

$$N_{OH} = 4.8 \times 10^{16} \text{cm}^{-2} \left(\frac{m_c}{0.02 M_\odot} \right) \left(\frac{X_{OH}}{10^{-3}} \right) \left(\frac{s}{r} \right) \\ \times \left[\left(\frac{\tau_{evap}}{2 \times 10^8 \text{yr}} \right) \left(\frac{f_\Omega}{0.25} \right) \left(\frac{r}{2.6 R_\odot} \right) \left(\frac{v_w}{200 \text{kms}^{-1}} \right) \right]^{-1} \quad (4)$$

This column density is indeed comparable to the values measured from the observed interstellar OH absorption towards pulsars (see Table 2).

To assess the column depth of N_{OH} in other binary pulsar systems listed in Table 1, we note that variables in Eq. (3) can be scaled to observable or listed parameters in Table 1. As before, we assume that $(s/r) \sim \text{constant}$. Furthermore Kluzniak et al (1988) derive \dot{M}_w as well as the evaporative wind velocity v_w driven by total γ -ray radiation and TeV e^\pm pairs radiated by the pulsar and intercepted by the secondary when the binary pulsar enters the present phase of radio pulsar driven evaporation of the secondary in PSR B1957+20. Using these expressions, we estimate: $N_{OH} \propto L_\gamma^2 r^{-5} h R_c^2$, where L_γ is the MeV γ -ray luminosity, R_c is the companion radius intercepting a fraction of that luminosity at an orbital distance r , and h is the scale height of the companion's (inflated) atmosphere which may extend to a significant fraction of the Roche lobe. Since the engine of both the gamma-ray luminosity as well as the TeV e^\pm luminosity is the spin down power of the neutron star, we can scale the column density of molecular OH in terms of the pulsar parameters as: $N_{OH} \propto \dot{E}^2 / P_{orb}^{10/3}$. For parameters listed in Table 1, the highest N_{OH} is predicted for the original black widow pulsar PSR B1957+20, but the N_{OH} for the first 3 entries of Table 1 are within an order of magnitude of that predicted for PSR B1957+20.

The red back "candidate transitional" pulsar PSR J1723-2837 has a mean flux density (at 1400 MHz) of 1.1 mJy as listed in ATNF catalog. However with an orbital period 14.76 hrs the column density of N_{OH} could be low. This pulsar may be a good candidate in the upcoming SKA era for attempts to detect OH/HI lines, but is likely to be challenging with present telescopes if its flux remains steady. The transitional millisecond pulsar PSR J1227-4853 (Roy et al. 2015) with shorter orbital period and significant \dot{E} has been found to eclipse at 1420 GHz (Parkes) and at 607 MHz (GMRT). Its continuum flux density at 607 MHz is 6.6 mJy; assuming a spectral index of -1.7 used by Roy et al. (2015), the estimated flux at 1420 MHz would be 1.6 mJy, which may also pose a

⁶ The timescale of ablative mass loss from the system can be directly calculated from the orbital period evolution (Czerny and King 1988; Fruchter et al 1990). However, The orbital period of PSR B1957+20 is undergoing small, apparently random variations on 5 yr timescale (Nice et al 2000) which *may be* related to the quadrupolar deformation of the magnetically active secondary with a sizeable convective envelope. The secondary may undergo a wind driven mass loss, which is powered by tidal dissipation of energy and a torque on the companion (Applegate and Shaham 1994). Lazaridis et al. (2011) argue that for PSR J2051-0827 gravitational quadrupole and classical spin-orbit coupling can together account for its observed orbital variations if the companion is underfilling its Roche-lobe by only a moderate factor, e.g. with a radius $R_c = 0.14 R_\odot$. The orbital period change of millisecond pulsar PSR J1744-24A implies a timescale of $|P_{orb}/\dot{P}_{orb}|_{obs} = 200$ Myr and the residual pulsar timing noise in these binary systems is interpreted as due to mass flow in the system (Nice et al 2000).

challenge for atomic and molecular line detections even if its column depth of molecular OH could be significant.

4.3. Atomic Hydrogen HI in the binary system?

If both molecular OH and neutral atomic hydrogen are present in the gas ablated from the ultra-low mass companion of the energetic pulsar, one can also estimate the possible column depths. If the X_{OH} fraction is slightly subsolar, e.g. $\sim 10^{-3}$ as we have assumed above, the column depth of HI in the intrabinary gas, assuming much of the gas is made of hydrogen and hydrogen is locked up mostly in atomic form (HI) once the gas cools down to temperature ~ 100 K, and scaling the N_{OH} column depth in Eq. (3) yields $N_{HI} \sim (5 - 10) \times 10^{19} \text{cm}^{-2}$. Given the relation between column depth and the EW for HI absorption (Kulkarni & Heiles 1988): $N_{HI} = 1.8 \times 10^{18} \langle 1/T_s \rangle^{-1} EW$ where $\langle 1/T_s \rangle^{-1}$ is harmonically weighted spin temperature along the path, whose value may be 50-100 K, one finds $EW \sim 2 \text{km s}^{-1}$. One can detect such EW's in the *pulsar spectrum* easily. Note that variations in column densities of $\sim 10^{18-19} \text{cm}^{-2}$ have been detected on occasions towards strong pulsars like PSR B1929+10 (Weisberg & Stanimirović 2007; Stanimirović et al. 2010). This gives an indication of the scale of measurable HI column depths in ISM and the estimated $N_{HI} \sim (5 - 10) \times 10^{19} \text{cm}^{-2}$ derived from Eq. (3) can therefore be detected.

5. OBSERVATIONAL REQUIREMENTS

The strategy for the detection of molecular line absorption (or emission) in the intervening medium probed by the narrow beam of pulsar radiation involves two primary considerations. First, the pulsed flux of radiation should be high enough for easy detection in narrow radio frequency bands that are fine enough to sample the absorption line *width* sufficiently well. The linewidth is determined by a combination of thermal broadening and microturbulence in the absorbing gas, – the latter is due to many small cells of gas moving in random directions with a Maxwellian distribution of speeds, leading to a Gaussian line profile (which is however independent of the mass of the absorbing atom or molecule, in contrast to the thermal width which varies $\propto m^{-1/2}$). Moreover due to binary companion's motion and the speed of the ablated tail wind, the centroid of the spectral line may move over a relatively wider range, compared to thermal line width. Even though one would like to determine the line profile, the narrow line width is a challenge since resolving the line requires high spectral resolution and given a pulsar flux density, the required signal to noise for pulse detection scales with frequency bandwidth as: $\propto (\Delta f)^{1/2}$. However, even when a line profile cannot be measured with great precision due to spectral resolution issues, equivalent width⁷ and curve of growth analysis

⁷ The equivalent width, W_ν , or W_λ , that measures the strength of the absorption line is the width of the adjacent continuum that has the same area (in the plot of the radiance per unit frequency or wavelength vs frequency or wavelength) as taken up by the absorption line. $W(\lambda_0) = \int_{-\infty}^{\infty} [1 - \exp(-\tau(\lambda - \lambda_0))] d\lambda$, and $W_{\nu_0} = (c/\lambda_0^2) W_{\lambda_0} = \int_{-\infty}^{\infty} [1 - \exp(-\tau(\nu - \nu_0))] d\nu$. When τ_ν is small across the line, as in the optically thin case, the equivalent width is linearly proportional to the column depth of the absorbing atoms or molecules along the line of sight (Spitzer 1978).

(Spitzer 1978) have been used to deduce gas temperature, column density and abundance of elements. Second, the sensitivity of the spectral measurement should be high enough to adequately sample the flux inside the absorption *depth* for the expected column of the atoms or molecules along the line of sight. That is, it should yield the equivalent width of the absorption line with sufficient accuracy. The sensitivity to measuring small equivalent widths of absorption lines improves directly with resolving power, provided adequate signal to noise can be achieved in the continuum neighboring the lines (Black 2005).

5.1. Equivalent width of the absorption line

Measurement of absorption spectra of interstellar HI and OH against the pulsed radiation has been described in Koribalski et al. (1995); Stanimirovic et al. (2003); Weisberg et al (2005) (see especially the supporting on-line material of the last reference). Briefly, a correlation spectrometer is used in the pulsar binning mode wherein each correlation function was recording into one of 2^N (e.g. 32) pulse phase bins that resulted in 2^N phase binned spectra covering a radio frequency bandwidth (e.g. 4 MHz for Parkes telescope, subdivided into 2048 spectral channels typically ~ 2 kHz or ~ 0.4 km s $^{-1}$ wide). The spectra obtained in the phase bins that had the pulsar pulse were collapsed into a single ‘‘pulsar-on’’ spectrum. Similarly, the spectra recorded for off-pulse phase bins were integrated into a single ‘‘pulsar-off’’ spectrum. The so-called *pulsar spectrum* was formed from the difference of *pulsar-on* and *pulsar-off* spectra and normalized by the mean pulsar flux. A frequency switching that takes the central radio frequency away from the line was used to flatten the baseline. This method of constructing the *pulsar spectrum* removes any in-beam molecular or atomic line *emission* due to the broad telescope beam and measures the pulsar signal alone absorbed by any intervening OH in intrabinary or interstellar medium.

We estimate the typical exposure requirements for Green Bank Telescope (GBT) if it were to be used for OH line detection from pulsars similar to those listed in Table 1. We note that all pulsars listed in Table 1 have typical *mean* S1400 flux densities of 3-4 mJy (except the one in globular cluster NGC6544, namely PSR J1807-2459A). These pulsars also have a 10% duty cycle, which implies that the peak flux during the pulse on phases will be approximately 10 times higher, although the pulse on phase is only 1/10th the pulsar full period. The radiometer equation gives the sensitivity of a radio telescope and receiver system to pulsed signals in terms of a threshold flux density S_{mean} (Lorimer & Kramer 2012):

$$S_{mean} = \beta \frac{(S/N)_{mean} T_{sys}}{G \sqrt{n_p t_{int} \Delta f}} \sqrt{\frac{W}{P - W}}, \quad (5)$$

where T_{sys} is the system noise temperature (including sky and receiver noise), G the telescope gain to convert between temperature and flux density (in the Rayleigh Jeans limit), n_p is the number of orthogonal polarizations summed in the signal, t is the integration time for the pulsar observation, Δf is the observing bandwidth, $(S/N)_{mean}$ is the threshold signal to noise for detection, W is the ‘pulse on’ duration, P is the pulse period (rotational period of the neutron star), and $\beta \simeq 1$ denotes

a factor of imperfections due to the digitization of the signal in the receiver system and other effects.

For a pulsar with a mean flux 3 mJy and a signal to noise ratio $(S/N)_{mean} \sim 9$ (see discussion after Eq. (8)), observed with GBT⁸, Eq. (5) can be rewritten as:

$$\frac{t_{int}}{5 \text{ hr}} = \left(\frac{T_{sys}}{16 \text{ K}}\right)^2 \left(\frac{G}{2 \text{ K/Jy}}\right)^{-2} \left(\frac{S_{mean}}{0.2 \text{ mJy}}\right)^{-2} \left(\frac{W/P}{0.1}\right) \times \left[\left(\frac{n_p}{2}\right) \left(\frac{\Delta f}{0.4 \text{ km/s}}\right)\right]^{-1} \quad (6)$$

The minimum detectable flux for a given pulsar (with P and W) is usually set by the threshold signal to noise ratio (S/N) . But since we are interested in absorption line profile in the *pulsar spectrum*, which flux are we referring to? If we set S_{mean} to be the continuum flux of the *pulsar spectrum* outside the channels occupied by the absorption line, the flux there is relatively high. However, what matters for line profile determination is that our flux uncertainty should be low enough to measure the *residual* between the continuum S_c (assumed to be constant over a narrow line width say of Gaussian profile⁹) and the flux density at the line center (where the optical depth is τ_0) with a high enough significance. Since the absorption of pulsed radiation in the OH band is variable with time due to the pulsar orbital motion, the determination of its magnitude can be limited by the errors arising out of short exposure times. The equivalent width for the absorption line itself (for a Gaussian line) can be written as:

$$EW = 1.06 \tau_0 FWHM$$

The equivalent width can be written in terms of the flux density in the continuum $F_c(\lambda)$ and in the line $F(\lambda)$ in a wavelength interval $\lambda_1 < \lambda < \lambda_2$ (outside this regime $F(\lambda) = F_c(\lambda)$) as:

$$EW_\lambda = \Delta\lambda - \int_{\lambda_1}^{\lambda_2} \frac{F(\lambda)}{F_c(\lambda)} d\lambda$$

where $\Delta\lambda = \lambda_2 - \lambda_1$. By applying the mean value theorem this can be re-expressed as (Vollmann & Eversberg 2006):

$$EW_\lambda = \Delta\lambda \left[1 - \frac{\overline{F(\lambda)}}{F_c(\lambda)}\right]$$

where $F_c(\lambda)$ is measured outside the line region and interpolated across the line where the absorption is taking

⁸ The parameters of the GBT L-band Receiver listed in Eq. (6) can be found in Table 3 and Fig 3 of the GBT Proposers Guide at: <https://science.nrao.edu/facilities/gbt/proposing/GBTp>. The actual time reported on the left hand side of Eq. (6) has been calculated using the Sensitivity Calculator for VEGAS spectrometer at: https://dss.gb.nrao.edu/calculator-ui/war/Calculator_ui.html. This is based on the assumption that the typical duty cycle has $W/P \sim 0.1$. Calculated exposure time depends upon several factors, e.g. whether signal and reference observations are differenced, the ratio of observing time on signal and reference, etc. The time reported in Eq. (6) does not difference signal and reference observations. Continuum flux is also measured in ‘‘signal’’ observations.

⁹ In terms of the spectrometer bandwidth, a Gaussian profile with line broadening ξ_m due to microturbulence and thermal broadening has $FWHM = 1.6652(\nu_0/c)\sqrt{(2kT/m + \xi_m^2)}$.

place and the overbars denote the average value of a variable. Both $F(\lambda)$ and $F_c(\lambda)$ have statistical errors. If their errors are not correlated, then their standard deviations can be determined separately. On the other hand the error estimate of the equivalent width of a spectral line has been derived by Vollmann & Eversberg (2006). The overall uncertainty of the EW is determined by two factors: the photometric uncertainty of the system and the uncertainty of the continuum estimation over the line. For low absorption line fluxes Vollmann & Eversberg (2006) show that the standard error of the equivalent width $\sigma(EW_\lambda)$ can be written as:

$$\sigma(EW_\lambda) = \frac{(\Delta\lambda - EW_\lambda)}{(S/N)} \times \left[1 + \frac{\overline{F_c}}{\overline{F}}\right]^{1/2}$$

where the relevant S/N ratio is the S/N in the undisturbed continuum and $\Delta\lambda$ is a measure of the line width in wavelength units. For weak lines, i.e. where the depth of the line is very small, $\overline{F} \sim \overline{F_c}$ and the above relation reduces to:

$$\sigma(EW_\lambda) = \sqrt{2} \frac{(\Delta\lambda - EW_\lambda)}{(S/N)}$$

This then leads to, using $\Delta\lambda - EW_\lambda = \Delta\lambda(\overline{F}/\overline{F_c})$,

$$\frac{EW_\nu}{\sigma(EW_\nu)} = (S/N) \frac{EW_\nu}{\Delta\nu} \times \left[\frac{\overline{F}}{\overline{F_c}} \left(1 + \frac{\overline{F}}{\overline{F_c}}\right)\right]^{-1/2} \quad (7)$$

where $\Delta\nu = (c/\lambda^2)(\lambda_2 - \lambda_1)$. Here $(S/N) = (S/N)_{mean}$ is determined by the observational and telescope parameters as in Eq. (5). For weak or low absorption line strengths, one has $\overline{F} \sim \overline{F_c}$, and the flux dependent factor in square brackets in Eq. (7) is about $1/\sqrt{2}$. Similarly the ratio of FWHM to $\Delta\nu$ that arises out of the ratio $(EW_\nu/\Delta\nu)$ is also of the order of unity. Therefore given a τ_0 the significance of the line detection in terms of its equivalent width is:

$$\frac{EW_\lambda}{\sigma(EW_\lambda)} \approx 0.3 \left(\frac{\tau_0}{0.3}\right) (S/N)_{mean} \quad (8)$$

Against the very bright pulsar-on phase, it will be relatively easier to measure the changes in the flux density in the OH-line profile, since the high flux density at a specific frequency channel can be relatively easily determined. The local continuum of the *pulsar spectrum* can be determined much more accurately than in the line absorption frequency channels, since many more channels (compared to where the line is located) can be averaged together in the continuum during data processing to get a good $(S/N)_{mean}$. If the absorption in the 1667 MHz band has, for example, an optical depth at the line center $\tau_0 = 0.3$ then the significance of the EW measurement would be lower than that of pulse detection in the continuum part of the *pulsar spectrum*. With increasing τ_0 , the equivalent width will be determined at a significance $(S/N)_{mean}$ approaching the pulsar signal detection itself (in the continuum). Thus to effect a detection of the absorption line with a similar τ_0 (and with $(EW/\Delta EW) = 3$), one requires a significance of detection of the *pulsar spectrum* of $(S/N)_{mean} \sim 9$ while for deeper absorption lines (with higher τ_0), a significant detection of the OH absorption line may be effected at even a lower $(S/N)_{mean} \sim 3-5$. Our estimate of the telescope resource requirements before (e.g. Eq. (6)) however is

based on the conservative case of moderate absorption depths and line-widths.

The dip in the flux density would decrease towards the absorption line wings over a velocity range whose magnitude could be similar or somewhat larger than the thermal speed (about 0.4 km s^{-1}) of the OH gas, i.e. about $2-3 \text{ km s}^{-1}$ (we note that Minter (2008) gives the FWHM for PSR B1718-35 OH absorption in the *interstellar medium* to be about 3 km s^{-1} at 1667 MHz; in the binary system, the wind speed from the companion and the OH line width is likely to be larger). The orbital velocity scale is typically several 100 km s^{-1} for a system like PSR B1957+20, although because of the mainly tangential swept back wind, the velocity width in the radiatively connected region along the line of sight is likely to be substantially smaller. Thus, the OH absorption to orbital phases near the eclipse may be distributed over a velocity width $\leq 10 \text{ km s}^{-1}$. Note that since only times close to the total eclipse would have substantial OH absorption, only that fraction of the orbital period (e.g. the $\sim 50^m$ periods around ingress and egress for PSR B1957+20) are relevant and the required total exposure have to be distributed over these epochs. Since these periods last together about 10-15% of the full orbital phase (for the case of PSR B1957+20), the total exposure time has to be spread over many orbital cycles. Finally, it will be efficient to use a sufficiently large bandwidth of the spectrometer in several spectral windows to cover all L-band OH lines (1612-1720 MHz) and HI line simultaneously.

Thus, each pulsar listed in Table 1 (first four rows) requires about 5 hrs of telescope time with the typical sensitivity of GBT. Pulsars in the declination range $0-40^\circ$ are accessible to Arecibo, which is most sensitive existing telescope. In fact, GBT, Arecibo, and Parkes Radio Telescope each detected one of the pulsars listed in Table 2. Future telescopes like the Square Kilometer Array (SKA) will have typically ten (SKA1-Mid) to hundred times (full SKA) flux sensitivity compared to GBT. With SKA-1 increased sensitivity in L-band (Band3) using low noise amplifiers, it will be possible to carry out such molecular line detections down to a pulsar mean flux density level of 0.7 mJy or lower, opening up several other known pulsar targets for similar studies. In addition, many newly discovered pulsar targets will become available for studies of composition of the winds from the companion.

5.2. Search for gas in a binary pulsar system through gated spectral line interferometry

So far our discussion of absorption spectroscopy in the *pulsar spectrum* has been in the time (pulsar rotational phase) vs radio frequency domain and in the context of single dish telescopes. In section 4.1 we have discussed that detection of orbital phase modulation can distinguish the intrabinary atomic/molecular gas from the circumbinary gas or that in the interstellar medium. By employing multiple antenna dishes in an interferometer, it is also possible to add a third domain, namely spatial information in the plane of the sky. While it is not possible at present to spatially resolve a binary system at the relevant distances of pulsars, any detection of molecular or atomic gas (through absorption or stim-

ulated emission) coincident with the pulsar position can be expected to be associated with the binary system if it is point like and spatially coincident. This is especially so if the pulsar occurs out of the galactic plane where the occurrence of such gas clouds is rarer in the interstellar medium. The primary advantage offered by interferometric line absorption studies is the ability to resolve out the foreground neutral atomic/molecular line emission and thus yield an uncontaminated measure of the absorption line profile that traces gas in the narrow beam subtended by the background source (in this case the pulse-on phase of the pulsar radiation). Moreover, it is possible with interferometric systems to achieve high spectral dynamic range, which opens up the possibility of measuring small optical depths, which can probe a Warm Neutral Medium (WNM) (Roy et al. 2013). Weisberg & Stanimirović (2007) showed that for PSR B1849+00 whose line of sight passes near the edge of the SNR Kes 79 had far smaller optical depth for OH absorption in the pulsar-off phases than in the pulsar-on OH spectra ($\tau(1667\text{MHz}) = 0.02$ vs 0.9), which they explained as the pulsar-Earth pencil beam of radiation having intercepted dense ($> 10^5 \text{ cm}^{-3}$) and small (typical angular size $< 15''$) cloudlets in the pulsar ISM spectra. In the pulsar-off spectrum, the sampling of absorption is across the full telescope beam that represents a larger solid angle average across a clumpy ISM consisting of high optical depth, small molecular cloudlets embedded in lower density medium.

As is well known, the significance of detection of a pulsating point source can be largely improved by removing the off-pulse noise. A background sky subtraction procedure for the pulse on - pulse off “gated” image constructed by an interferometer (such as the ATCA, (Camilo et al. 2000)) can unambiguously identify the location of the pulsed emission. Millisecond pulsars (MSPs, discovered by *Fermi* with poor spatial information) which require high time resolution for the gating procedure have been localized to an accuracy of $\pm 1''$ in the *on - off* gated image plane at GMRT. GMRT observations use a coherently de-dispersed gating correlator of the multiple antenna outputs that accounts for, at the same time, orbital motions of the MSPs while interferometer visibilities are folded with a topocentric rotational model derived from periodicity search simultaneously with the beamformer output (Roy & Bhattacharyya 2013). The positional accuracy of even the faint MSPs obtained from the *on-off* gated image improve with the S/N of the pulsar detection. Even though at 322 MHz, the GMRT synthesized beam has a positional accuracy of FWHM $10''$, an accuracy of $\pm 1''$ has been obtained for the timing position of the pulsar with a S/N of 5, and the astrometric accuracy accelerates the convergence in pulsar timing models for newly discovered pulsars such as the *Fermi* MSPs (Roy & Bhattacharyya 2013). This reduces the telescope time requirements for subsequent follow-up timing observations and reduces the effect of large covariances in the timing fit between pulsar position and spin period derivative, \dot{P} . While GMRT cannot observe in the OH bands, it can do so in the HI (1420 MHz) band. For example, GMRT interferometric observations of Galactic HI 21cm absorption spectroscopy towards 32 compact bright extragalactic radio sources (with L-band flux greater than 3 Jy)

have led to the detection of Warm Neutral Medium of spin temperature of several thousand degrees K (Roy et al. 2013). In the HI band these observations achieved typically a velocity resolution of $\sim 0.4 \text{ km s}^{-1}$ and a velocity coverage of $\sim 105 \text{ km s}^{-1}$ by using a single IF band with two polarizations and a baseband bandwidth of 0.5 MHz subdivided into 256 channels.

At the VLA, THOR - The HI, OH, Recombination Line Survey of the Milky Way has been undertaken to study atomic, molecular and ionized emission of Giant Molecular Clouds (GMC) in our galaxy (Bihr et al. 2015). These observations are interferometric (e.g. the Pilot survey for HI from GMC W43 was in the C-array of VLA) and have high spectral resolution (channel width of 1.953 kHz, with $\Delta v \sim 0.41 \text{ km s}^{-1}$ in the HI 21cm line, while that for OH lines for the region around the same target the channel spacing was 0.73 km s^{-1} at 1612 MHz (Walsh et al. 2016)). The synthesized beam size was of the order of $20'' \times 20''$ but the absolute positional accuracy of a point source with a 5σ detection would be: $\Theta_{\text{Beam}}/2\sigma = 2''$. Thus, the VLA C-array and GMRT would achieve similar spatial resolutions for OH/HI bands centered around a target binary MSP at about 1 kpc, with $\sim 0.01 \text{ pc}$ spatial scale. Since spatial densities of molecular or HI clouds along a narrowly defined line of sight towards high galactic latitude are likely to be small, a detection of absorbing gas is likely to be physically associated with the pulsar system itself, especially if the column densities are high.

The typical rms noise in THOR Pilot survey was 19 mJy/beam for the OH lines and 9 mJy/beam for the HI band which was achieved in 8 min pointing of the VLA. The survey has not exploited any underlying time dependent structure (e.g. a pulsar) of the spectral line signal. As we argue in section 5.1, for a pulsar of mean flux density of 3 mJy being obscured by companion wind of optical depth $\tau \sim 0.3$, a typical 10σ signal for the pulsar continuum required for adequate line detection would lead to 1σ rms of 0.3 mJy. If there were no pulsed signal, such a low rms could be achieved with the VLA if we scale the THOR exposure (8 min) by the ratio of the square of the respective flux rms, to obtain an overall exposure of $(19 \text{ mJy}/0.3 \text{ mJy})^2 \times 8 \text{ min} = 534 \text{ hr}$. However, for a MSP with a duty cycle that is 10% of its spin period, if we can (phase)gate the pulsar signal and construct the *pulsar on - off spectra* as described before we will gain a factor of 1/10, thus reducing the exposure requirement to about 53 hr. This is still too large for a single pulsar target. While such a capability may not exist at present for the OH band, the HI line transitions may be more promising, requiring about 12 hr of exposure (with similar scaling and assumptions of optical depth in the HI line absorption), provided adequate hardware and computational resources are available.

6. DISCUSSION

Molecular line detection would indicate the presence of constituent elements in the vicinity of the planet or the ultra-low mass companion. An Oxygen rich atmosphere could indicate a CO degenerate core of a helium burnt star as the companion. A simultaneous detection of neutral hydrogen and OH lines would indicate whether the gas has solar metallicity or has metals which are substantially super-solar, as might be the case if the companion's

external surface which may have once contained substantial fraction of hydrogen is stripped off of its external layers. Detection of OH lines or the atomic hyperfine transition line of ${}^3\text{He}^+$ (${}^2S_{1/2}, F = 0 - 1$) at 8.665 GHz would lead to constraints on the present state, e.g. the mass and radius of the companion.

The OH molecule is observed in a variety of astrophysical systems, including comets and the ISM. OH is usually formed by the dissociation of H_2O molecule, so it is often considered a proxy for water. The rotational ground state of the OH molecule has four transitions: two “main” lines at 1667 MHz and 1665 MHz (with the largest Einstein A coefficients, e.g. $7.7 \times 10^{-11} \text{ s}^{-1}$) and two “satellite” ones at 1720 MHz and 1612 MHz (Rohlfs and Wilson 1996). The pumping mechanisms differ from one astrophysical system to another. In the case of comets, heating of their nuclei leads to evaporation of water and photo-dissociation due to solar radiation and the level population distribution is dominated by UV pumping by solar radiation. Absorption features in the solar spectrum can in some circumstances cause population inversion of the ground state. The 1665 and 1667 MHz main lines are often associated with star forming regions whereas the 1612 MHz lines are associated with evolved stars. All these lines are due to inversions arising through pumping of far-infra red photons. In contrast, the OH (1720 MHz) masers are pumped through collisions and far-IR radiation effectively causes the destruction of the population inversion required for maser action. A strong maser inversion for the OH (1720 MHz) line is collisionally excited at temperatures 30-120 K (Lockett et al 1999; Wardle 1999). If maser emission at 1720 MHz and absorption at conjugate frequency of 1612 MHz are detected, together these would constrain upper and lower limits of $(1 \times 10^{14} \text{ cm}^{-2})(\text{km s}^{-1})^{-1} < N_{\text{OH}}/\Delta v < (1 \times 10^{15} \text{ cm}^{-2})(\text{km s}^{-1})^{-1}$ when the gas column becomes thick to far-infra-red pump photons. When column densities higher than $(1 \times 10^{15} \text{ cm}^{-2})(\text{km s}^{-1})^{-1}$ are encountered this would lead to absorption in the 1720 MHz line (Weisberg et al 2005). Maser amplification requires large column densities of OH molecules ($10^{16} - 10^{17} \text{ cm}^{-2}$) with small velocity gradients. Frail (2011) has argued that such masers can occur preferentially where the observer’s line of sight velocity gradient is small, as in edge on geometries of transverse compressional shocks in supernova remnants interacting with molecular clouds.

The geometry of the pulsar driven swept back winds from the companions (as for example indicated by the pattern of dispersion measure related delays in the black widow pulsar PSR B1957+20) would also offer favorable geometry of small velocity gradients along the line of sight, especially in cases where the orbital speed of the companion is large. Therefore the detection of satellite lines in emission or absorption may probe the column density (velocity) gradients in the intrabinary region. Moreover, the search for OH absorption and possible detection of stimulated emission on timescales corresponding to duty cycles of millisecond pulsars will probe much shorter timescales of maser action by 2-3 orders of magnitude than known so far and may constrain the aspect ratios of the filamentary structures far beyond what are currently thought to be responsible for maser amplification in circumstellar or interstellar medium (Elitzur et al. 1991). Black widow and red back pulsars have the characteristics that make them good targets for OH line detection observations since pulsar timing and optical observations allow us to determine their geometry, including the eclipsing region, well and their short orbital periods allow for repeated observations over many orbits within reasonable timelines to build up gated exposure time on the radio pulses near eclipse ingress and egress.

7. ACKNOWLEDGEMENTS

We thank Mark Reid and Jonathan Grindlay for their comments on the manuscript. A.R. thanks Vicky Kaspi, Avinash Deshpande Sayan Chakraborti and Wlodek Kluzniak for discussions. He thanks the Fulbright Foundation for a Fulbright-Nehru Fellowship during a sabbatical leave from Tata Institute of Fundamental Research and thanks the Director and staff of the Institute for Theory and Computation, Harvard University for their hospitality during his visit. We acknowledge the use of Australia Telescope National Facility (ATNF) Pulsar Catalogue and Paolo Freire’s website on “Pulsars in Globular Clusters and the NASA Astrophysics Data System (ADS) search engines. We thank Nirupam Roy for discussions on spectral line interferometry for HI and OH lines and for pointing out the THOR pilot papers. We thank the referee Joel Weisberg for many insightful comments which helped us to improve the paper. We thank Thomas Tauris for his correspondence on the manuscript.

REFERENCES

- Alpar, M. A., Cheng, A. F., Ruderman, M. A., & Shaham, J. 1982, *Nature*, 300, 728
- Applegate, J. H. and Shaham, J. 1994, *ApJ*, 436, 312
- Archibald, A. M., Stairs, I. H., Ransom, S. M., et al. 2009, *Science*, 324, 1411
- Asplund, M. et al 2009, *ARAA*, 47, 481
- Bailes, M. et al 2014, *Science*, 333, 1717
- Banitt, M., Ruderman, M., Shaham, J. and Applegate, J. 1993, *ApJ*, 415, 779
- Bassa, C. G., van Kerkwijk, M. H., & Kulkarni, S. R. 2006, *A&A*, 450, 295
- Bednarek, W. 2015, *MNRAS*, 451, L55
- Bogdanov, S., Archibald, A. M., Bassa, C., et al. 2015, *ApJ*, 806, 148
- Bogdanov, S., Esposito, P., Crawford, F., III, et al. 2014, *ApJ*, 781, 6
- Benvenuto, O. G., De Vito, M. A., & Horvath, J. E. 2015, *ApJ*, 798, 44
- Buhr, S., Beuther, H., Ott, J., et al. 2015, *A&A*, 580, A112
- Black, J. 2005, *High Resolution Infrared Spectroscopy in Astronomy*, 3
- Breton, R. P., van Kerkwijk, M. H., Roberts, M. S. E., et al. 2013, *ApJ*, 769, 108
- Burton, M. G., Hollenbach, D. J., & Tielens, A. G. G. M. 1990, *ApJ*, 365, 620
- Caraveo, P. 2014, *Ann Rev. Astron. Astrophys.*, 52, 211
- Cayrel, R. 1988, *The Impact of Very High S/N Spectroscopy on Stellar Physics*, 132, 345
- Camilo, F., Kaspi, V. M., Lyne, A. G., et al. 2000, *ApJ*, 541, 367
- Chen, H.-L., Chen, X., Tauris, T. M., & Han, Z. 2013, *ApJ*, 775, 27
- Clifton, T. R., Frail, D. A., Kulkarni, S. R., & Weisberg, J. M. 1988, *ApJ*, 333, 332
- Crawford, F., Lyne, A. G., Stairs, I. H., et al. 2013, *ApJ*, 776, 20
- Czerny, M. and King, A. R. 1988, *MNRAS*, 235, 33P

- Deller, A. T., Moldon, J., Miller-Jones, J. C. A., et al. 2015, *ApJ*, 809, 13
- Doroshenko, O., et al. 2001, *A&A*, 379, 579
- Draine, B. T. 1978, *ApJS*, 36, 595
- Elitzur, M. McKee, C. and Hollenbach, D. 1991, *ApJ*, 367, 333
- Foster and Fischer 1996, *ApJ*, 460, 902
- Fruchter, A. S. et al. 1990, *ApJ*, 351, 642
- Fruchter, A.S. et al. 1988, *Nature*, 333, 237
- Frail, D. 2011, *Mem. S.A. It.*, 82, 703
- Freire, P. 2012, in *Neutron Stars and Pulsars: Challenges and Opportunities after 80 years, Proc. IAU Symposium No. 291*, ed. J. van Leeuwen
- Hewitt, J. W. Yusuf-Zadeh, F., Wardle, M. Roberts, D. A. & Kassim, N. E. 2006, *ApJ*, 652, 1288
- Hobbs, G. et al 2004, *MNRAS*, 352, 1439
- Istrate, A. G., Tauris, T. M., Langer, N., & Antoniadis, J. 2014, *A&A*, 571, L3
- Jia, K., & Li, X.-D. 2015, *ApJ*, 814, 74
- Kaplan, D. L., Bhalerao, V. B., van Kerkwijk, M. H., et al. 2013, *ApJ*, 765, 158
- Käuff, H. U. 2008, 2007 ESO Instrument Calibration Workshop, 131
- Keane, E., Bhattacharyya, B., Kramer, M., et al. 2015, *Advancing Astrophysics with the Square Kilometre Array (AASKA14)*, 40
- Keith, M. J., et al. 2011, *MNRAS*, 414, 1292
- Kerr, M., Johnston, S., Hobbs, G. and Shannon, R. M. 2015, *ApJ* 809, L11
- King, A. R., Davies, M. B., & Beer, M. E. 2003, *MNRAS*, 345, 678
- Koribalski, B., Johnston, S., Weisberg, J. M., & Wilson, W. 1995, *ApJ*, 441, 756
- Kluźniak, W., Ruderman, M. A., Shaham, J. and Tavani, M. 1988, *Nature*, 334, 225
- Kramer, M. et al. 1998, *ApJ*, 501, 270
- Kulkarni, S. R., & Heiles, C. 1988, *Galactic and Extragalactic Radio Astronomy*, 95
- Lazaridis, K., Verbiest, J. P. W., Tauris, T. M., et al. 2011, *MNRAS*, 414, 3134
- Lazaridis, K. et al 2009, *arXiv:0908.0285*
- Lazio, T. J. W. and Fisher, J. 2004, *AJ*, 128, 842
- Lin, D. N. C., Woosley, S. E. and Bodenheimer, P. H. 1991, *Nature*, 353, 827
- Lee, Y. S., Beers, T. C., Sivarani, T., et al. 2008, *AJ*, 136, 2022
- Lockett, P., Gauthier, E. and Elitzur, M. 1999, *ApJ*, 511, 235
- Lorimer, D. R., & Kramer, M. 2012, *Handbook of Pulsar Astronomy*, by D. R. Lorimer, M. Kramer, Cambridge, UK: Cambridge University Press, 2012, p. 265
- Lundgren, S. C., Zepka, A. F. & Cordes, J. M., 1995, *ApJ*, 453, 419
- Madhusudhan, N. et al 2014, *Protostars and Planets VI*, H. Beuther et al., p. 739
- Manchester, R. N. et al., 2005, *AJ*, 129, 1993
- Menou, K., Perna, R. and Hernquist, L. 2001, *ApJ*, 559, 1032
- Minter, A. H. 2008, *ApJ*, 677, 373
- Nicastro, L. et al. 1995, *MNRAS*, 273, L68
- Nice, D. J. et al. 2005, *ApJ*, 634, 1242
- Nice, D. J., Arzoumanian, Z. and Thorsett, S. E. 2000, *ASP Conference Ser.*, 200, 67
- Papitto, A., Ferrigno, C., Bozzo, E., et al. 2013, *Nature*, 501, 517
- Phinney, E. S. et al 1988, *Nature*, 333, 832
- Phinney, E. S., & Hansen, B.M.S., 1993, *ASP Conf. Ser.*, 36, 371
- Podsiadlowski, P. 1993, *ASP Conf. Ser.*, 36, 149
- Radhakrishnan, V., & Srinivasan, G. 1982, *Current Science*, 51, 1096
- Rasio, F. A., Shapiro, S. L. & Teukolsky, S. A. 1989, *ApJ*, 342, 934
- Ray, P. S. et al. 2014, *American Astronomical Society Meeting Abstracts* 223, 140.07
- Richer, H. B., Ibata, R., Fahlman, G. G., & Huber, M. 2003, *ApJ*, 597, L45
- Roberts, M. 2013, *IAU Symposium No. 291*, p. 127
- Rohlf, K. and Wilson, T. L. 1996, *Tools of Radio Astronomy* Chapter 14
- Romani, R. W. 2012, *ApJ*, 754, L25
- Roy, J., Ray, P. S., Bhattacharyya, B., et al. 2015, *ApJ*, 800, L12
- Roy, J., & Bhattacharyya, B. 2013, *ApJ*, 765, L45
- Roy, N., Kanekar, N., Braun, R., & Chengalur, J. N. 2013, *MNRAS*, 436, 2352
- Sigurdsson, S. et al., 2003, *Science*, 301, 193
- Spitzer, L. 1978, *Physical processes in the interstellar medium*, by Lyman Spitzer. New York Wiley-Interscience, 1978. 333 p. 52
- Stanimirović, S., Weisberg, J. M., Pei, Z., Tuttle, K., & Green, J. T. 2010, *ApJ*, 720, 415
- Stanimirovic, S. et al., 2003, *ApJ*, 592, 953
- Stappers, B. W., van Kerkwijk, M. H., Bell, J. F., & Kulkarni, S. R. 2001, *ApJ*, 548, L183
- Stappers, B. W. et al., 1996, *ApJ*, 465, L119
- Sternberg, A., & Dalgarno, A. 1995, *ApJS*, 99, 565
- Tauris, T. M., Kaspi, V. M., Breton, R. P., et al. 2015, *Advancing Astrophysics with the Square Kilometre Array (AASKA14)*, 39
- Tavani, M. and Brookshaw, L., 1992, *Nature*, 356, 320
- Thorsett, S. E., Arzoumanian, Z., & Taylor, J. H. 1993, *ApJ*, 412, L33
- van Dishoeck, E. F. 2014, *Faraday Discussions*, 168, 9
- Vollmann, K., & Eversberg, T. 2006, *Astronomische Nachrichten*, 327, 862
- Walsh, A. J., Beuther, H., Bühr, S., et al. 2016, *MNRAS*, 455, 3494
- Wang, Z. et al 2014, *ApJ*, 793, 89
- Wang, Z., Archibald, A. M., Thorstensen, J. R., et al. 2009, *ApJ*, 703, 2017
- Wasserman, I. & Cordes, J. M. 1988, *ApJ*, 333, L91
- Wardle, M. 1999, *ApJ*, 525, L101
- Weisberg, J. M. et al 2005, *Science*, 309, 106
- Weisberg, J. M., & Stanimirović, S. 2007, *SINS - Small Ionized and Neutral Structures in the Diffuse Interstellar Medium*, 365, 28
- Wolszczan, A. and Frail, D. 1992, *Nature*, 355, 145